OPEN-SOURCE OFDM WAVEFORM FOR RESEARCH AND EDUCATION ON EMERGING UNMANNED AERIAL COMMUNICATIONS SYSTEMS

Jaber Kakar (jaberk@vt.edu)[1], Jason Synder (snyder84@exchange.vt.edu)[1], Vuk Marojevic (maroje@vt.edu)[1], Carl B. Dietrich (cdietric@vt.edu)[1], and Jeffrey H. Reed (reedjh@vt.edu)[1]

[1]Bradley Dept. Electrical and Computer Engineering, Virginia Tech, Blacksburg, Virginia

ABSTRACT

The use of unmanned aircraft systems (UASs) for intelligence, surveillance and reconnaissance (ISR) applications is already of standard practice. More recently, a number of civilian use cases for UAS have been identified in the agriculture, entertainment, and exploration domains, among others. The successful integration of unmanned aircrafts in non-segregated airspace heavily relies on robust command and control communication links. However, as the missions of these aircrafts increasingly rely on the information exchange of rich-content data, usually captured by the aircraft sensors, the real-time transmission of payload data becomes a spectrum management problem. This paper analyses orthogonal frequency division multiplexing (OFDM) as a waveform for future direct ground-to-air links. We develop the physical-layer design parameters of an OFDM-based UAS waveform by means of simulations and present a highly flexible, open-source OFDM transceiver waveform for research and education in this emerging communications field.

1. INTRODUCTION

The use of unmanned aerial systems (UASs) for military intelligence, surveillance and reconnaissance (ISR) applications is of standard practice today. The applicability of UASs is, however, not limited to military ISR only, but also to a broad range of civilian use cases. Civilian applications can be of commercial or governmental nature [1] and include transportation and communications infrastructure for commercial industries on the one hand and humanitarian and public safety for national governments on the other. Public safety applications, for instance, include disaster management (chemical sensing, flood monitoring, wildfire management, etc.), search and rescue missions, and surveillance (border and coastal/maritime patrol, traffic monitoring, etc.) [2, 3]. Recent predictions, conducted by the US National Transportation Center, reveal that the number of unmanned aerial vehicles (UAVs) for non-military purposes will exceed 200,000 [4]. Economy of scale will likely happen for micro and small UAVs with sizes of less then 10 feet and weights below 55 pounds.

Increasing UAV densities will bring along challenges in sense and avoid (S&A), radio spectrum allocation [5] as well as UAV type-specific national airspace (NAS) integration [6]. A suitable waveform or waveforms need to be specified that provide robust communications links for critical command and control as well as spectral efficiency for throughput-intensive payload data. Recent work by Jain et al. [7] analyzes L-band digital aeronautical communication systems of Type 1 and Type 2 (L-DACS1 and L-DACS2) for UAS. L-DACS1 uses multi-carrier modulation similar to WiMAX, whereas L-DACS2 is similar to GSM. The authors suggest considering L-DACS1 over L-DACS2 because of the spectrum flexibility and efficiency of orthogonal frequency division multiplexing (OFDM) as well as OFDM's coexistence properties and interference avoidance techniques.

The huge success of OFDM in commercial cellular (LTE) and WLANs (802.11 family), in particular, has resulted in mature waveforms with support from academia (research) and industry (products). The inherent flexibility and implementation simplicity of OFDM, advances in interference cancellation and avoidance techniques together with sophisticated resource schedulers make OFDM waveforms a powerful component to satisfy today's wireless communications needs. Spectrum sharing may drive wireless communications of the future and OFDM is well suited for this application. The benefits for UAS are adaptive modulation and coding, dynamic resource allocation (for non-critical payload data) and the availability of systems with continuous R&D support from industry, government and academia.

We have created an OFDM transceiver waveform [8] to facilitate wireless communications education and research with focus on spectrum sharing and UAV communications. The open-source waveform is using frequency-division duplexing to transmit and receive using paired spectrum. Our waveform so far employs automatic repeat request (ARQ), using ACKs and NACKs along with configurable timeouts to guarantee payload delivery from a stationary base station node to a UAV node. Written in C++ using the liquid-dsp library, the waveform provides a flexible platform for research on communications system enhancements and spectrum management. The huge number of parameters allows for a wide variety of configurations. It efficiently runs on the Ubuntu operating system and accesses commercial off the shelf (COTS) SDR hardware.

The objective of this paper is analysing the suitability of OFDM for direct air-to-ground links and deriving suitable waveform parameters for reliable and spectrally-efficient communications system deployments (Section 3). The paper also introduces

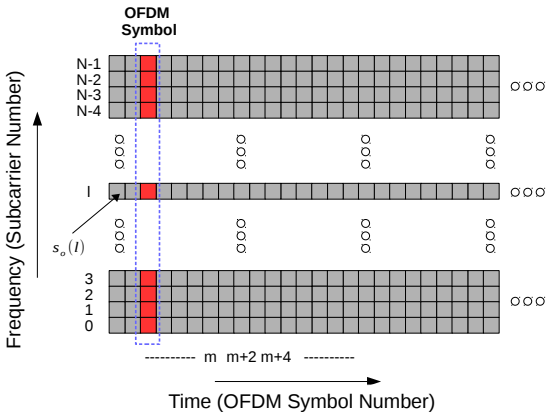

Figure 1: OFDM Time-Frequency Resource Grid.

our open-source OFDM waveform implementation to support research and education on new ways of spectrum management for UASs (Section 4). We conclude that OFDM is suitable for direct air-to-ground links and provide an outlook on UAS-related wireless communications research (Section 5). We provide a brief overview of OFDM first.

2. BACKGROUND ON OFDM

OFDM is a technique of modulating digital data on *multiple carriers*. This technique is used in broadband digital communications systems, such as 4G systems and digital video broadcasting.

Advantages of OFDM include tight channel packing when compared to conventional multi-carrier systems [9], resource allocation and sharing flexibility and ease of implementation when compared to single-carrier systems. In practical terms this typically leads to higher spectral efficiencies. The use of a cyclic prefix (CP) makes it possible to effectively eliminate inter symbol interference (ISI). Each OFDM subcarrier is an unfiltered waveform whose spectral sidelobes decay slowly. This brings along other challenges that are discussed in continuation.

2.1. Mathematical Description of OFDM

A single carrier modulated signal $s_c(t)$ of unit energy over a symbol period with center frequency f_c can be described by

$$s_c(t) = A_c(t)e^{j(2\pi f_c t + \Phi_c(t))}, \tag{1}$$

where $A_c(t)$ and $\Phi_c(t)$ result from amplitude and phase modulation. In case of OFDM, N subchannels or subcarriers are transmitted and result in the complex signal

$$s_o(t) = \frac{1}{\sqrt{N}} \sum_{k=0}^{N-1} A_k(t)e^{j(2\pi f_k t + \Phi_k(t))}, \tag{2}$$

where $f_k = f_0 + k\Delta f$. The modulation symbol interval is inversely proportional to the subcarrier spacing Δf to preserve orthogonality between subcarriers, avoiding inter-carrier interference (ICI) [10]. During a modulation symbol period, the phase and the amplitude components can be assumed to be constant, i.e. $A_k(t) = A_k$ and $\Phi_k(t) = \Phi_k$. Suppose the signal in (2) is sampled with sampling rate $f_s = 1/T_s$, then $s_o(lT_s)$ or simply $s_o(l)$ is the l-th sample of the baseband signal and is given by [11]

$$s_o(l) = \frac{1}{\sqrt{N}} \sum_{k=0}^{N-1} A_k e^{j\Phi_k} e^{j2\pi\Delta f k l T_s}. \tag{3}$$

The modulation symbol interval is then NT_s.

An OFDM symbol is defined in the time domain and, according to Figure 1, consists of N samples carrying N modulation symbols. (Note that the typical OFDM symbol definition includes the cyclic prefix, discussed later.) It is defined as $\{s_o(l)\}_{l=0}^{N-1}$. Comparing (3) with the definition of an Inverse Discrete Fourier Transform (IDFT) $x(l) = \mathcal{F}^{-1}\{X(k)\} = \sum_{k=0}^{N-1} X(k)e^{j2\pi lk/N}$, we determine $\Delta f = f_s/N$ for $X(k) = A_k e^{j\Phi_k}$. At the receiver side, we apply a Discrete Fourier Transform to obtain an estimate of $X(k)$. In practice, the computationally efficient IFFT and FFT is applied by means of zero padding, i.e., zero-valued modulation symbols, which constitute the guard bands.

2.2. OFDM with a Cyclic Prefix

The direct transmission of $s_o(t)$ through a finite-length dispersive channel with impulse response $h(t)$ will lead to loss of orthogonality at the receiver, leading to intercarrier and intersymbol interference (ICI and ISI). Adding a CP to an OFDM symbol of length similar to the delay spread effectively helps preserving orthogonality [11]. Suppose that we pass the CP-extended sampled signal

$$\tilde{s}_o(l) = \underbrace{[\underbrace{s_0(N-N_{CP})\cdots s_o(N-1)}_{\text{CP insertion}}, \underbrace{\{s_o(l)\}_0^{N-1}}_{\text{Initial OFDM Symbol}}]}_{\text{Overall Length } N+N_{CP}} \tag{4}$$

through a channel of N_h samples. The received signal will then look like

$$r(l) = \tilde{s}_o(l) * h(l) + n(l). \tag{5}$$

We can show that ISI is completely eliminated if $N_{CP} \geq N_h$, which means that at least N_h samples of $r(l)$ will be discarded before the OFDM demodulation [9]. The main disadvantage of CP insertion is that the transmit energy has to be increased by $\gamma_{CP} = (N + N_{CP})/N$ to achieve a desired Signal-to-Noise Ratio (SNR) [11]. In other words, CP insertion results in power loss as well as throughput loss since these samples are discarded at the receiver.

2.3. OFDM System Architecture

Figure 2 shows a basic OFDM communication system [12]. At the transmitter, the modulation symbols are applied to an N-point IFFT. The resulting samples are CP extended, before RF

processing. The receiver performs the reverse operations – CP detachment, N-point FFT – and channel estimation and equalization in the frequency domain, before demodulation and decoding.

The design of a reliable and spectrally-efficient OFDM communications system requires that the symbol duration T_s, number of subcarriers N and CP length N_{CP}, among others, be chosen as a function of the operational parameters (application requirements) and radio channel. This will be analysed in continuation.

3. UAV-TO-GROUND COMMUNICATION CHANNEL

The simplest communications system for a UAV operating in segregated airspace consists of the UAV and the ground control station (GCS) with exclusive frequency assignment for the direct UAV-to-GCS and GCS-to-UAV links, i.e., downlink and uplink. Such links can be line-of-sight (LoS) or over the horizon, or beyond-line-of-sight (BLoS). Without loss of generality, in this paper we assume LoS given that small UAVs (SUAV) and micro UAVs (MAV) with limited operational range will dominate the future airspace [4].

Keeping this trend in mind, it is expected that the (non-segregated) NAS will be heavily occupied by UAVs as well as manned aircrafts. To allow for safe integration of UAVs additional communications links to air traffic control (ATC) need to be established. A summary of all available ground-to-ground (G2G), air-to-air (A2A), air-to-ground (A2G) as well as ground-to-air (G2A) are provided in Figure 3 [13]. (Note that via-satellite links have been omitted according to the considered scope.) Critical for UAV airworthiness in NAS is the command & control or control and non-payload communications system, which needs to be highly reliable and of low latency. However, it is easy to imagine that the most throughput-intensive link will be the A2G payload link for real-time video broadcast or similar applications.

3.1. Generic Air-to-Ground Channel Model

The A2G channel with time-variant baseband channel impulse response (CIR) $h(t,\tau)$ in its most general form for a single-input single-output (SISO) antenna case is given by [14]

$$h(t,\tau) = \sum_{p=0}^{L(t)-1} \Big[z_p(t)\alpha_p(t) \underbrace{e^{j2\pi f_{D,p}(t)(t-\tau_p(t))}}_{\text{Doppler Effect}} \underbrace{e^{-j2\pi f_c(t)\tau_p(t)}}_{\text{Phase Shift}} \delta(\tau-\tau_p(t)) \Big], \quad (6)$$

where $L(t)$ is the number of multipaths, $\alpha_p(t)$ is the amplitude of the p-th multipath, $z_p(t) \in \{0,1\}$ is a persistence process to quantify the duration of multipath components (MPC), $f_c(t)$ is the carrier frequency (usually constant over time) and $f_{D,p}(t) = v(t)f_c(t)cos(\phi_p(t))/c$ is the Doppler-shift of the p-th multipath. The parameters $v(t), c$ and $\phi_p(t)$ are the relative aircraft-to-ground velocity, speed of light and the average angle of arrival for multipath component p. Typically we can observe that $f_c \gg |f_D|$, which means that exponential terms in Equation (6) change with significantly different rates.

The signal bandwidth B is important to differentiate different MPCs [14]. MPC spacing below $1/B$ is usually not traceable. A power delay profile (PDP) can be used to determine MPC delay spacing. We consider a channel as frequency-flat, as opposed to frequency-selective, if the coherence bandwidth B_c is greater than B. The coherence bandwidth is inversely proportional to the RMS delay spread σ_t [15]. For instance, considering a frequency correlation of 0.5 or greater as a measure of channel similarity will lead to an estimate of the coherence bandwidth as $\hat{B}_c = 1/(5\sigma_t)$. As bandwidth and symbol time T_s are also inversely proportional, a rule of thumb to detect flat-fading channels is $T_s > 10\sigma_t$.

The A2G channel in the time-domain can be evaluated by determining the coherence time T_c. The coherence time is reciprocally proportional to the Doppler shift f_D. T_c can be estimated from the maximal Doppler shift $f_{D,max} = vf_c/c$ as $\hat{T}_c = 0.423/f_{D,max}$ [15].

3.2. Typical A2G Channel Parameters

We are interested in wideband channel models for A2G in order to derive suitable OFDM waveform parameters. Table 1 summarizes the main measurement campaigns and their parameters. Several references from Table 1 do not explicitly specify the utilized bandwidth. The campaigns differ in deployed frequency, antenna configuration (including altitude) as well as the ground environment. Table 2 (parts based on [14]) summarizes the results for each measurement campaign in terms of the number of MPCs, RMS delay spread as well as the Doppler spectrum. Using the last two parameters, we are able to provide an estimate for coherence bandwidth and coherence time. A2G channel measurements in VHF frequecy range (30 MHz to 300 MHz) have for example been conducted in Aspen and Dulath [22] leading to (maximum) RMS delay spreads of about 4μs ($\hat{B}_{c,min} = 50$kHz). The RMS value in this case is more than 10 times higher than delay spreads for frequencies in L- and C-bands (see Table 2).

The results from Table 2 reveal that the RMS delay spread is a function of the aircraft and GCS altitude [18] or elevation angle [19]. The ground environment has an impact on the number of MPCs ([16] vs. [19]). This is in agreement with recent estimates for non-LOS (NLoS) probabilities for different ground environments [23, 24]. UAVs that operate at higher altitudes will usually produce a greater Doppler shifts than SUAVs and MAVs. The Different phases (parking, taxiing, take-off, landing, en-route) lead to different A2G channels. Measurements in [20] identify take-off and landing as the most critical phases because maximum delay spread (up to 34μs) as well as large Doppler spread (up to 2.5 kHz) are encountered.

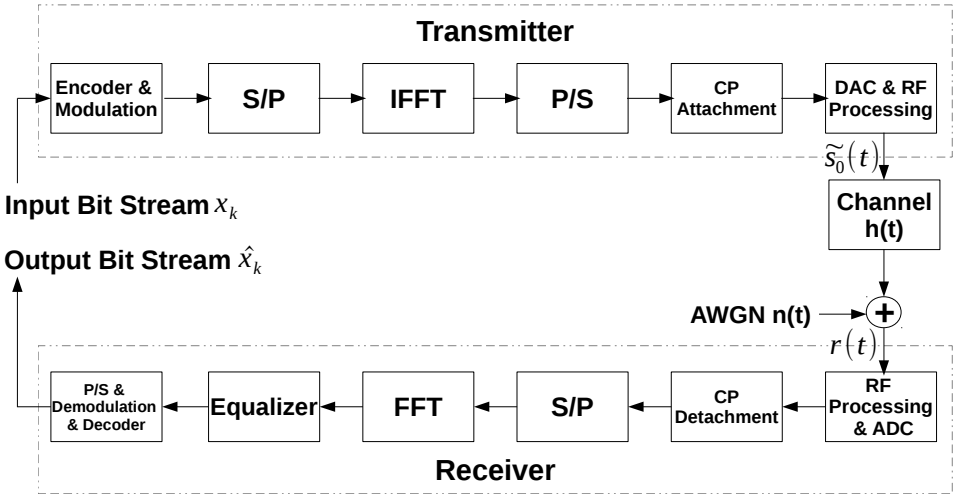

Figure 2: Physical layer processing blocks of a simple OFDM system, transmitter and receiver.

Table 1: Wideband Configuration for Air-to-Groud Measurements (Vertical Polarization)

Reference	**Frequency** [MHz]	**Antenna** (Elevation Beamwidth)				**(Antenna) Height** [m]		**Ground Environment**
		Aircraft		Ground Station		Aircraft	Ground Station	
		Omni.	Direc.	Omni.	Direc.			
[16]	1510.5 1460.5 2344.5 2360.5	√	×	×	6° 6° 3° 6°	1525/3050 AMSL	2.5 (Antenna) + 700 AMSL 2.5 (Antenna) + 700 AMSL 4.5 (Antenna) + 700 AMSL 2.5 (Antenna) + 700 AMSL	Mountainous Desert
[17]	5120	√	×	√	×	5000/8000/11000 AMSL	18 (Antenna) + 750 AMSL	Sonthofen (Germany)
[18]	5700	√	×	×	2 Antennas: 25°	370/970/1830	2.10 + ? 7.65 + ?	Sea Surface
[19]	2050	√	×	4-Array	×	$450 \leq h \leq 975$ AGL	GL	College Campus
[20]	5135	√	×	×	Dish (d=2.4 m)	Taxiing, Take-off, En-route	Airbus Saint-Martin site	Saint-Martin (Airbus)
[21]	960-977 5000-5100	×	Cosine	×	2 Antennas: 81° 2 Antennas: 35°	$h_{max} \approx 12,500$	3.5-18.3 + ?	Cleveland and Oxnard

Table 3: OFDM Design Equations

Design Equation	**Explanation**
$T_c > (N + N_{CP})T_s$	Variability in time negligible for OFDM Symbols
$(N + N_{CP})T_s \gg \sigma_t$	Avoidance of channel dispersion
$N_{CP}T_s > \sigma_t$	ISI prevention
$f_{D,max} \ll 1/(NT_s)$	Reduce Effect of ICI
$N_{CP}/N \ll 1$	Maintain high spectral efficiency
$\Pr(\text{PAPR} > \gamma) \leq \chi_{th}$	Keep likelihood of high PAPR low

3.3. OFDM Simulation

As already mentioned, for the design of a reliable, spectrally-efficient OFDM system, the sampling period T_s, number of subcarriers N and CP length N_{CP} need to chosen as a function of the operational requirements and conditions. We select T_s, N and N_{CP} [9, 14] to meet the design equations given by Table 3.

PAPR is the peak-to-average-power ratio given by [25]

$$\Pr(\text{PAPR} > \gamma) \approx 1 - \exp(-\alpha^{3/2} N e^{-\gamma} \sqrt{\rho\pi\gamma/3}), \quad (7)$$

where ρ the average power of active, i.e. non-zero, subcarriers, and αN the number of non-zero subcarriers to be used. We can rewrite the last design equation using Equation (7) to

$$\alpha^{3/2} N \leq -\frac{ln(1 - \chi_{th})e^{\gamma}}{\sqrt{\rho\pi\gamma/3}} \quad (8)$$

For $\gamma_{dB} = 10$ dB, $\rho = 1$ and $\chi_{th} = 5 \cdot 10^{-2}$, we the obtain $(\alpha^{3/2}N)_{min} \approx 349.13$. Assuming that more than 50% of all subcarriers are used for data or pilot tones, we obtain a maximum radix-2 FFT size $N_{max} = 512$. Maximum speeds of $v_{max} = 400$ km/h and a carrier frequency of $f_c = 5.1$ GHz lead to maximum Doppler shifts of about 1.9 kHz. Similar to LTE, we set the subcarrier spacing to $\Delta f \geq 15$ kHz.

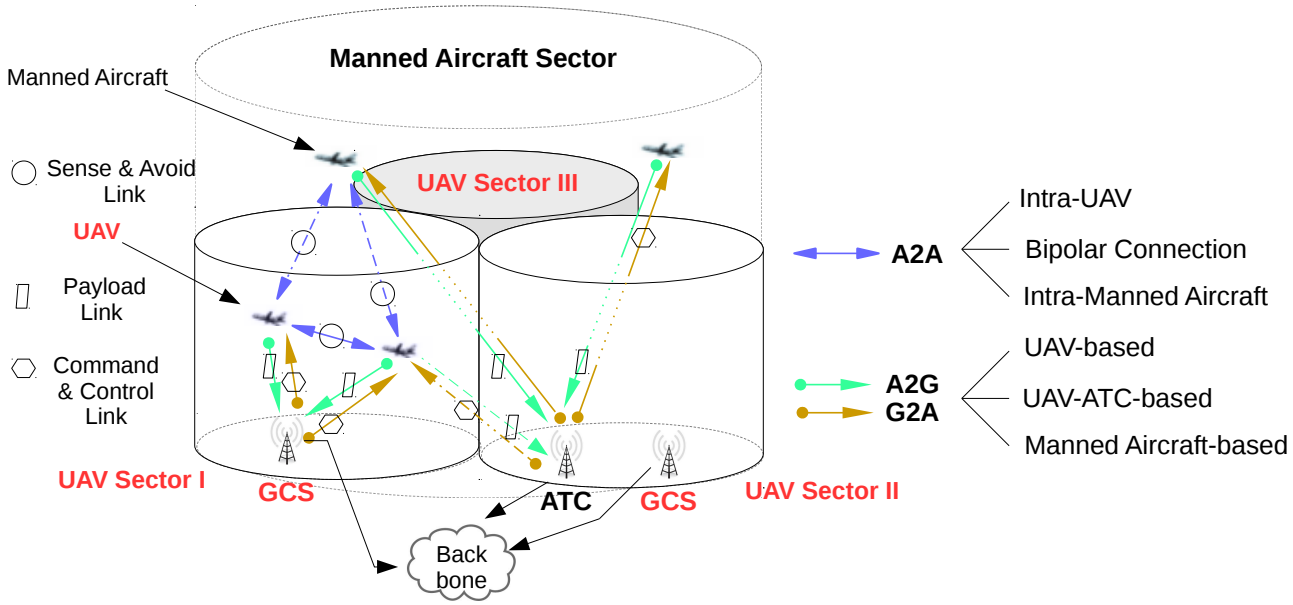

Figure 3: Potential LoS Link Architecture for Manned Aircrafts and UAVs in non-segregated airspace.

Table 2: Resulting (Estimated) Channel Parameters

Reference	$L(t)$		σ_t [μs]		**Doppler Spectrum** [kHz]	$\hat{B}_{c,min}$ [kHz]	$\hat{T}_c$ [μs]	**Comments**
	min	max	average	max				
[16]	3		0.074	–	–	–	–	–
[17]	1 (mainly LoS)		0.0384	0.398	$[-5; 5]$	≈ 500	≈ 85	v=±293 m/s,B=20 MHz STD(σ_t) ≈0.021 μs
[18]	2 or 3	7	–	0.480	–	≈420	–	Max RMS for Channel 2 (GCS Height: 2.10 m) and altitude 370 m
[19]	≈8		0.098[1]	0.485	–	≈410	–	Use of elevation angles θ: 7.5, 15, 22.5, 30°
[20]	1		–	–	$[-3.6; 4.1]$	–	≈105	Time Delay MPC for en-route not considered.
[21]	≈3		–	0.050	–	4000	–	For Oxnard C-band measurement case

Based on the existing literature, we have identified an approximate maximum excess delay spread of 2μs for low-altitude applications applicable to SUAVs and MAVs [19]. We use the per bin probability provided in Table 3 of reference [19] to extract the power delay profile (PDP) prototype defined by the delay vector $\tau = [0\ 33\ 70\ 115\ 175\ 262\ 405\ 682]$ ns and the normalized power vector $P_{dB} = [0\ -8.7\ -9.6\ -11.3\ -13.4\ -15.2\ -17.0\ -20.2]$ to simulate a 5 MHz wideband A2G channel for low-altitude operations. Assuming a 5 MHz channel bandwidth seems to be appropriate based on discussed frequency availability in the 960 MHz band [26].

We compute the bit error rate (BER) of an uncoded QPSK-modulated OFDM communications system for different waveform and channel parameters. The results are shown in Figure 4. Irrespectively of the carrier frequency, increasing the CP length from 8 to 15 does not improve the performance significantly as shown in Figure 4a. For an error rate of $P_b = 4 \cdot 10^{-3}$, we can observe a 3 dB gain when using a 2 GHz instead of a 5.1 GHz carrier frequency. The BER performance for $v = 40$ km/h and $f_c = 5.1$ GHz converges to $P_b = 5 \cdot 10^{-2}$ at relatively low E_b/N_0 (see Figure 4b). This performance can be improved to $P_b = 3 \cdot 10^{-2}$ if the number of used subcarriers is reduced by 50 % and the subcarrier spacing increased by 33 % (see Figure 4d). Based on Figure 4c, a decrease in the number of effective subcarriers N_u does not lead to a significant BER performance improvement. The selection of N_u is a trade-off between given spectrum mask and the spectral efficiency. Using a smaller amount of non-zero subcarriers will result in lower out-of-band transmission reducing adjacent band ICI at the cost of lower data rates.

4. UAV WAVEFORM

An open-source waveform was created to facilitate research and education on OFDM-based communication systems for UASs. The waveform was designed with a large number of configurable parameters that can be manually tuned by the user or

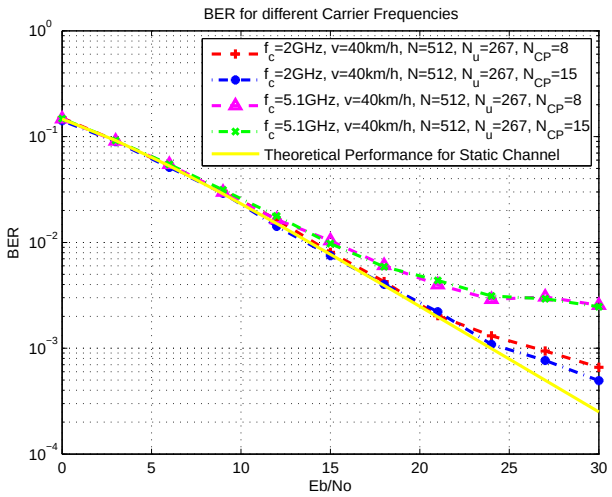

(a) Different Carrier Frequencies

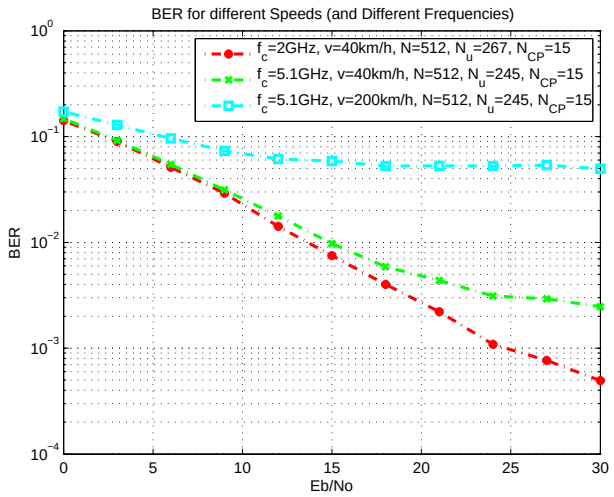

(b) Varying Speed and Carrier Frequency

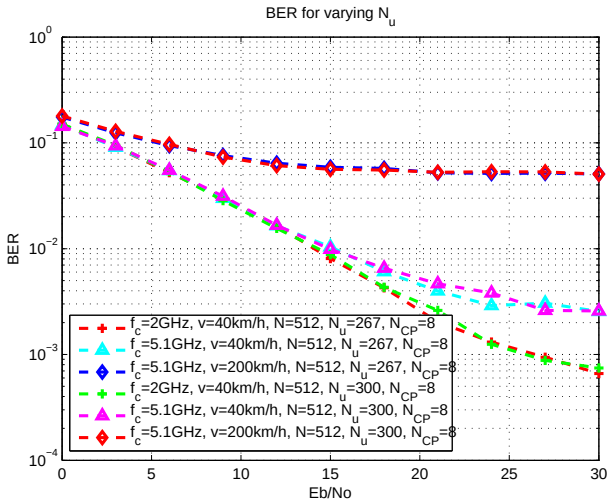

(c) Varying Number of non-zero Subcarriers

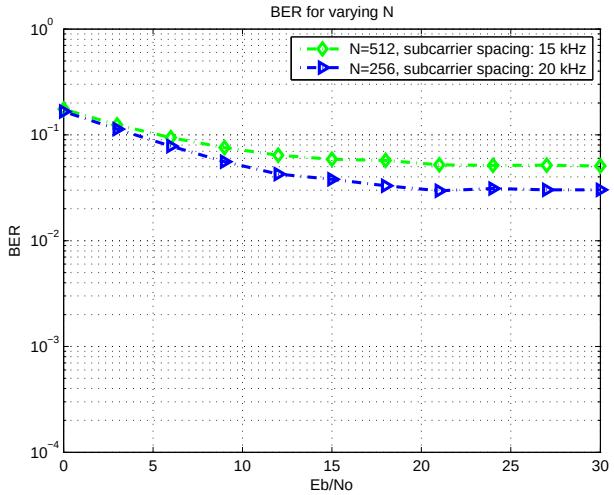

(d) Varying FFT size

Figure 4: BER Performance for different OFDM and Channel Parameters as a function of E_b/N_0

automatically adapted by schedulers or cognitive engines. The frequency-division duplex (FDD) mode was chosen for multiplexing uplink and downlink transmissions because of the large distances that the signals may travel. The waveform interfaces with Ettus Research USRPs [27] and is available for free download from [8].

4.1. Waveform Design

The waveform starts operates on packets to deliver from the GCS or any kind of base station to the UAV or vice versa. The GCS node transmits one packet, then waits a configurable amount of time (response_timeout) for a response from the UAV node. When the UAV node is able to detect and successfully decode the packet, it sends a small packet back to the GCS node to acknowledge correct reception. When the GCS receives the ACK, it contains the ID of the packet that was received by the UAV. The GCS then removes that ID from its list of packets to transmit. If the UAV is able to detect a packet but cannot decode it successfully, it will transmit a NACK packet back to the GCS. Upon receiving the NACK from the UAV, the GCS will immediately try to retransmit the packet. If no response is heard from the UAV within response_timeout seconds, the GCS will start a timer for the previous packet. Once that timer runs out after packet_timeout seconds, the GCS will retransmit the packet. The GCS continues like this, transmitting new and retransmitting old packets until it has received an ACK for every packet it transmitted. The UAV runs continuously, transmitting ACKs and NACKs to the GCS as appropriate, until it has not received any packets for a certain amount of time.

4.2. Code Design

The waveform was written using the C++ liquid-dsp and liquid-usrp digital signal processing libraries [28]. Specifically, it uses the *OFDMTxRx* class to handle packet transmission and reception. This class has many configurable parameters and allows the user or scheduler/cognitive engine to customize many options.

The set of system parameters have an effect on the ACK and NACK configuration. The main parameters are:

- Number of packets to transmit,
- Size of packets to transmit,
- Response timeout: waiting time before moving on to the next packet (default: 0.2 s),
- Packet timeout: waiting time before retransmitting a packet (default: 1 s),
- *RxTimeout*: UAV waiting time to shut down if no packets are received (default: 3 s).

The waveform parameters include modulation, coding and other transmission parameters:

- Uplink transmission frequency,
- Downlink transmission frequency,
- Bandwidth B,
- Software transmission gain,
- Hardware transmission gain (USRP specific gain),
- Hardware reception gain (USRP specific gain),
- Modulation scheme,
- Inner and outer forward error correction,
- Number of OFDM subcarriers N,
- Cyclic prefix length N_{CP},
- Number of non-zero subcarriers N_u.

By editing the open-source code, the user can precisely specify the subcarrier allocations, determine which subcarriers are used for data and which for pilots to assist in synchronization and equalization. The waveform can be extended with intelligent adaptation algorithms. For instance, for faster SUAVs, the FFT size as well as ACK/NACK timeout parameters can be reduced to improve the performance. The waveform has been tested on the the CORNET testbed [29] and on unmanned ground vehicles.

5. CONCLUSION

In the future, it is expected that commercial UAVs, particularly of type micro and small UAV, will be deployed in high quantities. Many applications require high throughput from the UAV to the GCS. Recent work [7] motivate the deployment of OFDM-based technologies. OFDM has good spectral efficiency, allowing to adapt to spectrum availability and channel characteristics. Computing efficient transceiver implementations exist that enable channel-specific adaptation. OFDM modulation is computationally inexpensive, but introduces delays due to block processing. OFDM-based waveforms pose a challenge to time and frequency synchronization as well as amplifier designs because of the high PAPR. OFDM relies on guard time and guard bands, leading to power and spectral inefficiency. Nevertheless, OFDM-based transceivers are widely adopted and supported and we believe that OFDM waveforms are very attractive for future communications systems integrated in low-cost MAVs and SUAVs.

We have proposed an open-source UAV waveform that can be used for further research in spectrum sharing and UAV communications. The waveform is highly flexible allowing changes, amongst others, in ACK/NACK configuration and OFDM parameters.

Based on the simulation results and A2G channel literature survey, we conclude that performance of OFDM waveforms for A2G channels can well be optimized by dynamically adjusting the waveform parameters as a function of operational and channel conditions. Speed, elevation angle, flight status (taxi, take-off, en-route, landing) and other parameters will suggest different waveform parameter sets. Adaptive radios and cognitive radios can, furthermore, exploit spectral opportunities in a congested spectrum for payload data. The spectrum assignments should take into account the type of UAV, vehicle speeds, etc. For example, high-speed vehicles operating at low-altitudes should be assigned lower frequencies than slower vehicles [26].

The existing waveform will be extended to account for aforementioned channel conditions and tested using our available testbed.

REFERENCES

[1] ITU, "Characteristics of unmanned aircraft systems and spectrum requirements to support their safe operation in non-segregated airspace," International Telecommunication Union, Tech. Rep. M.2171, December 2009.

[2] R. Austin, *Unmanned Aircraft Systems: UAVs Design, Development and Deployment*. Wiley, May 2010.

[3] R. E. Weibel and R. J. Hansman, "Safety Considerations for Operation of Unmanned Aerial Vehicles in the National Airspace System," Master's thesis, Massachusetts Institute of Technology, March 2005.

[4] John A. Volpe National Transportation Systems Center, "Unmanned Aircraft System (UAS) Service Demand 2015 - 2035," U.S. Department of Transportation, Tech. Rep. DOT-VNTSC-DoD-13-01, September 2013.

[5] P. E. Ross, "When will we have Unmanned Commercial Airliners?" *IEEE Spectrum*, November 2011.

[6] T. Simonite, "Air Traffic Control for Drones," *MIT Technology Review*, October 2014.

[7] R. Jain and F. Templin, "Requirements, challenges and analysis of alternatives for wireless datalinks for unmanned aircraft systems," *IEEE Journal on Selected Areas in Communications*, vol. 30, no. 5, pp. 852–860, 2012. [Online]. Available: http://dx.doi.org/10.1109/JSAC.2012.120602

[8] UAV Waveform Project Web Site. [Online]. Available: https://github.com/fr3lm0

[9] M. B. Stefania Sesia, Issam Toufik, Ed., *LTE – The UMTS Long Term Revolution*. Wiley, February 2009, ch. 5, pp. 111–113.

[10] W. Y. Y. C. G. K. Yong Soo Cho, Jaekwon Kim, Ed., *MIMO-OFDM Wireless Communications with MATLAB*. Wiley, October 2010, ch. 4, pp. 111–151.

[11] J.-J. van de Beek, P. O. Börjesson, P. Ödling, and S. K. Wilson, "Orthogonal frequency-division multiplexing (OFDM)," 1999.

[12] Z. Wu, H. Kumar, and A. Davari, "Performance Evaluation of OFDM Transmission in UAV Wireless Communication," *System Theory, 2005. SSST '05*, pp. 6–10, March 2005.

[13] S. Henriksen, "Unmanned Aircraft System Control and ATC Communications Bandwidth Requirements," NASA, Tech. Rep. 2008-214841, February 2008.

[14] D. W. Matolak, "Air-Ground Channels & Models: Comprehensive Review and Considerations for Unmanned Aircraft Systems," *IEEE Aerospace Conference*, pp. 1–17, March 2012.

[15] N. Tripathi and J. H. Reed, *Cellular Communications: A Comprehensive and Practical Guide*. New Jersey: Wiley, 2009.

[16] M. Rice, A. Davis, and C. Bettweiser, "Wideband Channel Model for Aeronautical Telemetry," *IEEE Transactions on Aerospace and Electronic Systems*, vol. 40, no. 1, pp. 57–69, August 2004.

[17] J. Kunisch, I. de la Torre, A. Winkelmann, M. Eube, and T. Fuss, "Wideband Time-Variant Air-to-Ground Radio Channel Measurements at 5 GHz," *European Conference on Antennas and Propagation (EUCAP)*, pp. 1386–1390, April 2011.

[18] Y. S. Meng and Y. H. Lee, "Measurements and Characterizations of Air-to-Ground Channel over Sea Surface at C-Band with Low Airborne Altitudes," *IEEE Transactions on Vehicular Technology*, vol. 60, no. 4, pp. 1943–1948, May 2011.

[19] W. G. Newhall, R. Mostafa, C. Dietrich, C. R. Anderson, K. Dietze, G. Joshi, and J. H. Reed, "Wideband air-to-ground radio channel measurements using an antenna array at 2 GHz for low-altitude operations," *Military Communications Conference*, vol. 2, pp. 1422–1427, October 2003.

[20] C. Blümm, C. Heller, B. Fourestie, and R. Weigel, "Wideband aeronautical channel sounding and modeling for C-band telemetry," in *PIMRC*. IEEE, 2013, pp. 264–269.

[21] D. W. Matolak, "AG Channel Sounding for UAS in the NAS," February 2014.

[22] G. Dyer, T. Gilbert, S. Henriksen, and E. Sayadian, "Mobile propagation measurements using CW and sliding correlator techniques," in *Antennas and Propagation Society International Symposium, 1998. IEEE*, vol. 4, June 1998, pp. 1896–1899 vol.4.

[23] A. Al-Hourani, S. Kandeepan, and S. Lardner, "Optimal LAP Altitude for Maximum Coverage," *Wireless Communications Letters, IEEE*, vol. PP, no. 99, pp. 1–1, 2014.

[24] J. Holis and P. Pechac, "Elevation Dependent Shadowing Model for Mobile Communications via High Altitude Platforms in Built-Up Areas," *Antennas and Propagation, IEEE Transactions on*, vol. 56, no. 4, pp. 1078–1084, April 2008.

[25] T. Jiang, M. Guizani, H.-H. Chen, W. Xiang, and Y. Wu, "Derivation of PAPR Distribution for OFDM Wireless Systems Based on Extreme Value Theory," *Wireless Communications, IEEE Transactions on*, vol. 7, no. 4, pp. 1298–1305, April 2008.

[26] R. Kerczewski, J. Wilson, and W. Bishop, "Frequency spectrum for integration of unmanned aircraft," in *Digital Avionics Systems Conference (DASC), 2013 IEEE/AIAA 32nd*, Oct 2013, pp. 6D5–1–6D5–9.

[27] Ettus Research. [Online]. Available: http://www.ettus.com/

[28] J. D. Gaeddert. liquid-dsp. [Online]. Available: http://liquidsdr.org/

[29] The Cognitive Radio Network (CORNET) Testbed. [Online]. Available: http://cornet.wireless.vt.edu/